Tziokas Nikolaos: MSc Student[1], Topouzelis Konstantinos: Assistant Professor[2] and Soulakellis Nikolaos: Professor[3]
[1,3]University of the Aegean – Department of Geography, [2]University of the Aegean – Department of Marine Sciences
[1]geom17027@aegean.gr, [2]n.soulakellis@aegean.gr , [3] topouzelis@marine.aegean.gr

Use of Object Based Image Analysis in very high-resolution images to evaluate buildings damage after an earthquake: The case of Vrysa settlement, Lesvos island

Abstract

This study presents the methodology followed for the evaluation of buildings damage after the earthquake of 12th of June in Vrysa, Lesvos island. For this purpose, VHR multispectral images from a flight from a UAS were acquired. The methodology consisted of two main steps. Firstly, through the orthorectification and radiometric calibration procedure, a multispectral orthophotomap was created. The final result was classified hierarchically using object-based Image Analysis (OBIA). The first hierarchical level divides the area into two major classes, natural and structured habitat, while at the second level both of them included various subcategories. In order to better distinguish categories and enhance classification, several spectral indices and ratios have been calculated and integrated into the model. The results show that very high multispectral images (VHRMSI) in combine with fuzzy rules can provide reliable information on building damage after an earthquake. Also, the use of object-based Analysis in conjunction with spectral indices, ratios and nDSM has optimized the precision of the classification. The overall accuracy of the classification was 87%.

Keywords

UAS, VHRMSI, OBIA, fuzzy rules, classification

Introduction

A natural disaster such as an earthquake, can potentially cause from building damages to the loss of human lives. Following the earthquake, there is an extreme need of surveying the damages in the affected area in a quick and trustworthy way. This enables to provide instant aid to the people affected by it. Satellites and other aerial media such as UAS, are the commonly used media which provide the information for surveying. Both of them can provide VHR images which can be used when mapping the damaged of a compound. Some other ways for surveying the building damages are the use of photogrammetry methods (Altan et al., 2001), 3D laser scanner (Block et al., 2016) and fieldwork.

Object-based image analysis is called the analysis on an image on an object level and not on a pixel level (Blaschke et al., 2014). Vu, Matsuoka & Yamazaki (2005) used the object-based

analysis method in order to locate the buildings which were damaged by comparing multispectral images before and after the earthquake. Gusella et al. (2005) used multispectral satellite images after the earthquake for surveying the damaged buildings and they applied the object-based analysis, ultimately the estimate in categories was accurate by 85%. Khudhairy, Caravaggi & Giada (2005) using VHR images of the satellite Ikonos, applied object-based analysis method in order to estimate the structural damages. Bitelli & Gusella (2008) recognized the importance of multispectral images and images with high spatial resolution for managing natural disasters. Also, they insist on the importance of the object-based analysis method for instant surveying of buildings' construction, in order to effectively apply risk management.

This particular study aims to estimate and map the effect of the earthquake on the compound of a part of a traditional settlement located in Vrysa, Lesvos. The estimate was accomplished by using the object-based analysis method in multispectral high-resolution images which were captured by an unmanned flight with UAS. This paper organized in four parts. Part one is the study area and the data collection. In part two we apply orthorectification and the object-based methodology. In the third part we discuss in an in-depth manner the results of the proposed methodology. Finally, in the fourth part, are the conclusions.

Area of study and data collection

Vrysa is a traditional settlement, geographically located on the southern part of Lesvos Island. The buildings of the village are mainly made either of stone or concrete (Kiratzi, 2018). According to the last census occurred in 2011, the population of the village was 798 residents (Municipality of Polychnitos, 2017). The villages stand between two normal active crevasses (Kiratzi, 2018). The data used were obtained from one UAS, in which a camera Parrot Sequoia was placed. This camera has a sensor with spectral technical characteristics collected from 5 channels. One channel captures in the visible wavelength and the rest 4 in red, green, red edge and near infrared wavelengths. The technical details about the camera are shown on the table 1.

Table 1: Characteristics of the Parrot Sequoia camera, (https://www.micasense.com/parrotsequoia, 2017)

MSC	**SEQUOIA**	
CATEGORY	MS	RGB
LENSES	4	1
RESOLUTION (pixels)	1280x960	4608x3456
PIXEL SIZE (μm)	3.75	1.34
WAVELENGHTS	NARROWBAND	BROADBAND
SPECTRAL RANGE	530-810	400-700
BANDWIDTH	10-40	100

For this study were used 300 multispectral pictures with 80% overlap and 70% sidelap. The points for georeferencing which were used are 4. For the illustration of the locations of GCPs in Vrysa, GPS ProMark3 RTK was used, manufactured by Magellan, which belongs to the

Cartography and Geoinformatics laboratory of the Geography department. ProMark3 RTK consists of 2 sensors (Base and Rover) and it had all the necessary equipment for RTK and PostProcessing applications, including a pair of transceiver radio modem.

Methodology

The first stage of the study was to edit the multispectral images in order to create a multispectral orthophotomap. Orthophotomap is called a map on which the area of study is depicted in orthographic projection and includes cartographic elements (Perakis et al, 2013). The second step was to apply the object-based analysis method using the multispectral Orthophotomap. The aim of using the object-based analysis method was to obtain a classified map. The following diagram (Figure 1) depicts the steps which were followed until the accuracy assessment of the classified map.

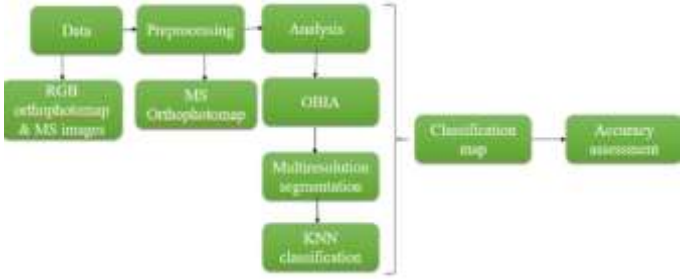

Figure 1: Flowchart of the methodology

The first stage of the methodology was to edit the multispectral images. Ultimately, after editing the images an Orthophotomap was created. The editing process in particular was the radiometric correction and the orthorectification. The second stage, was the use of the object-based image analysis method. The main characteristic of this method is the segmentation of the image in objects, which form the analysis unit of the method (Gusella et al., 2005). The objects are consisting of pixels with common characteristics. Generally, the object-based analysis method is consisted of two steps. The first step is the segmentation of the images into objects and the second step is to classify the objects. Also, there is an option of creating multiple segmentation levels.

Preprocessing

The first part of editing was the radiometric correction of the multispectral images. The goal of this was to correctly estimate the percentage of the reflected radiation (Teillet, 1986). Parrot Sequoia has one calibration target which is used to correct the multispectral images. For each calibration target, a mask had to be created around it, in order to clear the part of it which was irrelevant to the calibration plate (Agisoft Photoscan Manual, 2018). 4 calibration

plates were used, one per channel. In this way, the actual percentage of the target's radiation is recorded. The aforementioned editing procedure was used across all the channels.

Since the georeference system of the images used was in WGS '84, it had to be deleted from the images and then to be transferred to the Greek Geodetic System of Reference. The georeference locations which were available were in EGSA '87. Firstly, the locations to be georeferenced were chosen. Secondly, was the procedure of recognizing each location of these on the images. Lastly, the relevant error was assessed. The relevant error, following the georeference, was measured to 0,03m.

Next the product had to be orthorectified, so the images were merged and created a sparse point cloud. The sparse point cloud was turned into a dense point cloud. Through triangulating of the points, a grid was created ending up in connecting all the points in a dense cloud. After that the texture was edited and the Digital Surface Model was created having 0.05 m spatial resolution. Also, the nDSM (DSM-DEM) was calculated, which was used later in the classification (Appendix, Map 1). Finally, the multispectral Orthophotomap which was created had pixel size 0.05m (Appendix, Map 2).

Analysis

For the segmentation of the Multiresolution segmentation algorithm was applied. This algorithm belongs to the region-based techniques (Chen, 2007) and takes into consideration 4 parameters. The weight of each channel, the Scale parameter, the Shape parameter and the Compactness parameter. The Scale parameter is a mixture of the Shape and Compactness parameters. Also, the Scale parameter is defining the common size of the objects' disunion (Benz et al., 2004; Zhang, Maxwell, 2006). The values given to each of the parameters in every segmentation level is shown on the below table (Table 2).

Table 2: Parameters of the Multiresolution segmentation

Scale	10, 20
Shape	0.3
Compactness	0.5
Bands	1: Red, Green, Red Edge, NIR, nDSM

According to table 2, there are 2 segmentation levels. The first one corresponds to the Scale parameter which equals 20. For the second level, the Scale parameter equals 10. In this way, a hierarchical semiotic network was created (Benz et al., 2004). This means that each object knows the adjacent to it objects and the objects from which it derived. The bands which were used are the Red, Green, NIR, Red Edge και nDSM channels. The numbers next to each channel (Table 1) state the weight of each band during the segmentation.

The second stage of the analysis procedure was the classification. Firstly, 4 categories, or so called super categories, were created. Secondly, for each one of the 2 super categories,

there was a subcategory defined. In this way the hierarchical structure was done. In the hierarchical structure each subcategory has the characteristics of the initial category (Antunes et al., 2003).

First of all, 4 big categories were chosen, Artificial areas, Forest and semi natural areas, Bright areas και Shadows. The categories were chosen in accordance with the level 3 and 2 land cover of Corine (Corine 2000) using subtle changes. For the category Artificial areas another 4 subcategories were created: The Continuous urban fabric, Ruins, Roads/Paved land and Other constructions. For the category Forest and semi natural areas 3 subcategories were created: Bare soil, Natural grassland and Trees. For the categories Bright surface και Shadows the same subcategories were created.

The algorithm chosen for the classification was the k-Nearest Neighbor (kNN) in combination with the use of the fuzzy rules. The kNN belongs to the category of fuzzy logic (Villar et al., 2016) and it is a soft classifier. It classifies the objects according to the adjacent training samples (Kim et al., 2012). The big advantage of the algorithm is the simplicity (Gadwe et al., 2016). Furthermore, eight fuzzy memberships functions were created aiming to create fuzzy rules. The fuzzy rules were to be useful during classification, because the differences of the objects could not be defined by the spectral indices and ratios

Additionally, 350 more objects were classified manually. Finally, the objects which belonged to the same category were merged, in order to create bigger and less objects.

Table 3: The spectral indices & ratios which used

NIR/RED	GREEN/RED
NDVI	GREEN NDVI
GREEN/NIR	WVI
RED/GREEN	NDRedEdgeI

Results

The radiometric correction of the images helped the extraction of quantitative information, which means to calculate the spectral indices and ratios.

For DSM, the size of the grid was selected to 5 cm in order to provide the best way to capture the structures contained in the relief.

The multispectral orthophotomap had spatial resolution 5cm (Appendix, Map 1). In this way the ruins and the damages of the buildings could be observed. The cartographic representation of both the Natural and Artificial environment was made possible. However, at the areas which are located at the borders of the image, the resolution was worse compared to the rest of the image. The problem lies in the fact that the targets, when identifying them in the process of binding, were identified in less than 9 photographs. This complicates the visual interpretation of the situation in which those areas are.

Image segmentation applied at 2 times in order to generate meaningful objects. A critical point is the separation of the Bare soil from other Artificial areas. Their difference was

at the GR NDVI spectral index (unclassified with GR NDVI [-0.13,0.06] classify it as Bare soil). The first segmentation had Scale parameter 20 thus larger objects were obtained. This led to objects that contained different pixels with differences in their spectral signatures. For this reason, the objects were resegmented and as an optimum Scale parameter the value 10 was selected. For this level of the segmentation the Shape and Compactness parameters had values of 0.9 and 0.5 respectively. The choice of these values was made though visual interpretation. Figure 2 shows illustrates the categories which created at the 2nd level of segmentation and the hierarchical network.

Figure 2: Class hierarchy & categories

In all spectral indices and ratios, the spectral signature of the objects is almost identical. In order to discriminate the 2 categories, the relationship with their super categories was used.

For the classification process the kNN algorithm was selected. For the super-category, which had Scale parameter 20, a total of 120 samples were selected. The classification was based only on the spectral signatures of the objects in the various spectral indices and ratios. For the sub-category, which had Scale parameter 10, the classification was based also on their spectral signature, but the relation with the super-category was used. Also, a total of 8 fuzzy rules were used.

Because the surface of the area is quite complicated, the manual classification was necessary. In particular, 3 houses which are located at the South part of the study area and could not be identified by the nDSM, were initially classified as Bare soil. Through visual interpretation those objects were identified and reclassified. The other case where manual classification was deemed necessary was that of the Ruins into Roads/Paved surfaces. In the areas where the Road borders with the bare ground, the algorithm classified them as Ruins. This happened for two reasons. Firstly, because those borders, in the super-category, were classified as Artificial areas. The result is those borders remained unclassified in the sub-category, when Bare ground was classified. Second, because the boundaries of Roads / Paved land and Bare soil are closer, spectrally to those of the Ruins class, about 430 objects were classified as Ruins. Again, through visual inspection these areas were identified and reclassified. The last reclassification case concerned the Continuous urban fabric category whose roofs suffered total collapse. The result was that only the outline of the houses could be identified visually, while the inside of the house would appear to be a shaded area. These houses were reclassified manually from the Shadow category to the Ruins category. Figure 3 below shows the final classification after joining the objects.

Figure 3: The map of the classification

The image shows the 9 categories in which the objects were classified. It is noted that most Ruins are located in the central and northern part of the study area (red color). The south-eastern part of the study area appears to have the least damage. Totally, 1009 Ruins polygons were counted. The category of the Ruins has a 5% of the number of the total objects in the image.

Accuracy assessment occurred after the analysis of the categories. Table 4 (Appendix, Table 4) shows the Error Matrix. The percentage of the Overall accuracy was 87%. For the category of Ruins, the Producers and Users accuracy was 0.73 and 0.97 respectively. Of the 49 samples selected for accuracy assessment, 36 of them were correctly classified, while the remaining 11 were classified as Shadows and Other constructions. Finally, the number of samples selected for each category is proportionally equal to the number of objects created. The final map of classification (Appendix, Map 3) is shown an area located in the North of the study area, which was affected the most by the earthquake.

Conclusions and discussion

The conclusions arise from this paper are mainly four. Firstly, UAS gives the possibility to capture fast and accurately an area affected by an earthquake. Also, the affected area can be recorded safely. Secondly, the process of producing multispectral orthophotomap is relatively quick and simple. Thirdly, automation of the identification of the damaged buildings is a complex issue, thus use of spectral indices, thematic layer and other type of information is critical concerning the classifications accuracy. Also, using a hierarchical network and inheriting attributes between categories makes the process of classifying objects fast and efficient. Comparing to other studies, the proposed methodology managed to achieve very high accuracy rates. In the future, the thermal orthophotomap will be used, which will be produced by the Parrot Sequoia thermal channel combined with the thematic level of the roads. Finally, the quantification of goodness of segmentation and morphological factors will be applied in a next level.

Acknowledgements

This research would not be completed over a six-month period without the help of the postgraduate student of Drolia Garyfallou Chrysovalanti on theoretical issues of georeference. Also, I would like to thank Mr. Papaconstantinou Apostolo for the data he provided. Finally, I would like to express my warmest thanks to Professor Ms. Briassouli Helen and the candidate PhD. Gounaridi Dimitrio for the guidance they gave me regarding the writing of a scientific article. The DEM was given to the researcher by the Cartography Laboratory of the Department of Geography. Finally, I would like to thank Tsikaderi Ismini and Mitsi Terpsichori for the help they provided for the English syntax of the paper.

References

Agisoft (2017), Multispectral image calibration and processing in PhotoScan Pro 1.4, Manual

Al-Khudhairy D.H.A., Caravaggi I., Giada S. (2005) Structural Damage Assessments from Ikonos Data Using Change Detection, Object-Oriented Segmentation, and Classification Techniques, *Photogrammetric Engineering & Remote Sensing*, Vol. 71, No. 7, pp. 825–837

Altan O., Toz G., Kulur S., Seker D., Volz S., Fritsch D., Sester M. (2001) Photogrammetry and geographic information systems for quick assessment, documentation and analysis of earthquakes. *ISPRS Journal of Photogrammetry & Remote Sensing*. 55. 359–372

Antunes A. F. B., Lingnau C., Centeno J. A. C. (2003) Object oriented analysis and semantic network for high resolution image classification, v. 9, no 2, p.233-242

Benz U. C., Hofmann P., Willhauck G., Lingenfelder I., Heynen M. (2004) Multi-resolution, object-oriented fuzzy analysis of remote sensing data for GIS-ready information, *Journal of Photogrammetry & Remote Sensing*, 58, 239– 258

Bitelli G., Gusella L. (2008) Remote sensing satellite imagery and risk management: image-based information extraction, *Transactions on Information and Communication*, Vol 39

Blaschke T., Geoffrey J. H, Kelly M., Lang S., Hofmann P., Addink E., Queiroz R. F., Meer F., Werff H., Coillie F., Tiede D. (2014) Geographic Object-Based Image Analysis – Towards a new paradigm, *Isprs Journal of Photogrammetry and Remote Sensing*, 87(100): 180–191

Bloch T., Sacks R., Rabinovitch O. (2016) Interior models of earthquake damaged buildings for search and rescue. *Advanced Engineering Informatics*. 30. 65–76

Chen D. (2007) Optimization in multi-scale segmentation of high-resolution satellite images for artificial feature recognition, *International Journal of Remote Sensing*, Vol. 28, No. 20, 4625–4644

Corine (2018). Available at https://land.copernicus.eu/pan-european/corine-land-cover/clc-2012 [Access at 11/3/2018]

Gadwe K., Waghchoure N., Gokule S., Reddypatil H., Vharkate M. (2016) Remote Sensing Image Classification Using kNN Algorithm, *IJSRSET*, Volume 2, Issue 2, 2394-4099

Gusella L., Adams B. J., Bitelli G., Huyck C. K., MEERI, and Mognol A. (2005) Object-Oriented Image Understanding and Post-Earthquake Damage Assessment for the 2003 Bam, Iran, Earthquake, *Earthquake Spectra*, Volume 21, No. S1, pages S225–S238

Jhan J.-P., Rau J.-Y., Huang C.-Y. (2016) Band-to-band registration and ortho-rectification of multilens/multispectral imagery: A case study of MiniMCA-12 acquired by a fixed-wing UAS, *Journal of Photogrammetry and Remote Sensing*, 114, 66–77

Kim H., Kim B-S., Savare S. (2012) Comparing Image Classification Methods: K-Nearest-Neighbor and Support-Vector-Machines, Applied Mathematics in Electrical and Computer Engineering

Kiratzi A. (2018) The 12 June 2017 Mw 6.3 Lesvos Island (Aegean Sea) earthquake: Slip model and directivity estimated with finite-fault inversion. Tectonophysics. 724–725, 1–10

MicaSense (2017). Available at https://www.micasense.com/parrotsequoia/ [Access at 22/11/2017]

Teillet P. M. (2007) Image correction for radiometric effects in remote sensing, *International Journal of Remote Sensing*, VOL. 7, NO. 12, 1637-1651

Villar P., Montes R., Maria A. S. Herrera F. (2016) Fuzzy-Citation-KNN: a fuzzy nearest neighbor approach for multi-instance classification, International Conference on Fuzzy Systems (FUZZ)

Vu T. T., Matsuoka M., Yamazaki F. (2015) Towards an object-based detection of earthquake damaged buildings, Commission VII, WG VII/5

Zhang Y., Maxwell T. (2006) A fuzzy logic approach to supervised segmentation for object-oriented classification, ASPRS, Annual Conference Reno, Nevada

Municipality of Polychnitos (2017). Available at http://www.vatera.gr/ [Access at 10/11/2017]

Appendix

Table 4 : Error Matrix of the classification

User Class \ Sample	Continues urban fabric	Trees	Grassland	Bare land	Shadows	Bright surfaces	Other constructions	Ruins	Road/Paved land	Sum	User
Continues urban fabric	33	0	0	0	0	0	0	0	0	33	1
Trees	0	27	1	0	0	0	0	0	0	28	0.96
Grassland	0	1	6	1	0	0	0	0	0	8	0.75
Bare land	0	0	1	16	0	0	0	0	2	19	0.84
Shadows	0	0	0	0	45	0	0	5	1	51	0.88
Bright surfaces	0	0	0	0	0	0	3	0	2	5	0
Other Constructions	4	0	0	0	0	0	40	6	3	53	0.75
Ruins	0	0	0	1	0	0	0	36	0	37	0.97
Road/Paved land	0	0	0	0	0	0	2	2	24	28	0.86
Unclassified	0	0	0	0	0	0	0	0	0	0	
Sum	37	28	8	18	45	0	45	49	32		
Producer	0.89	0.96	0.75	0.89	1	undefined	0.89	0.73	0.75		
Overall Accuracy	0.87										
KIA	0.84										

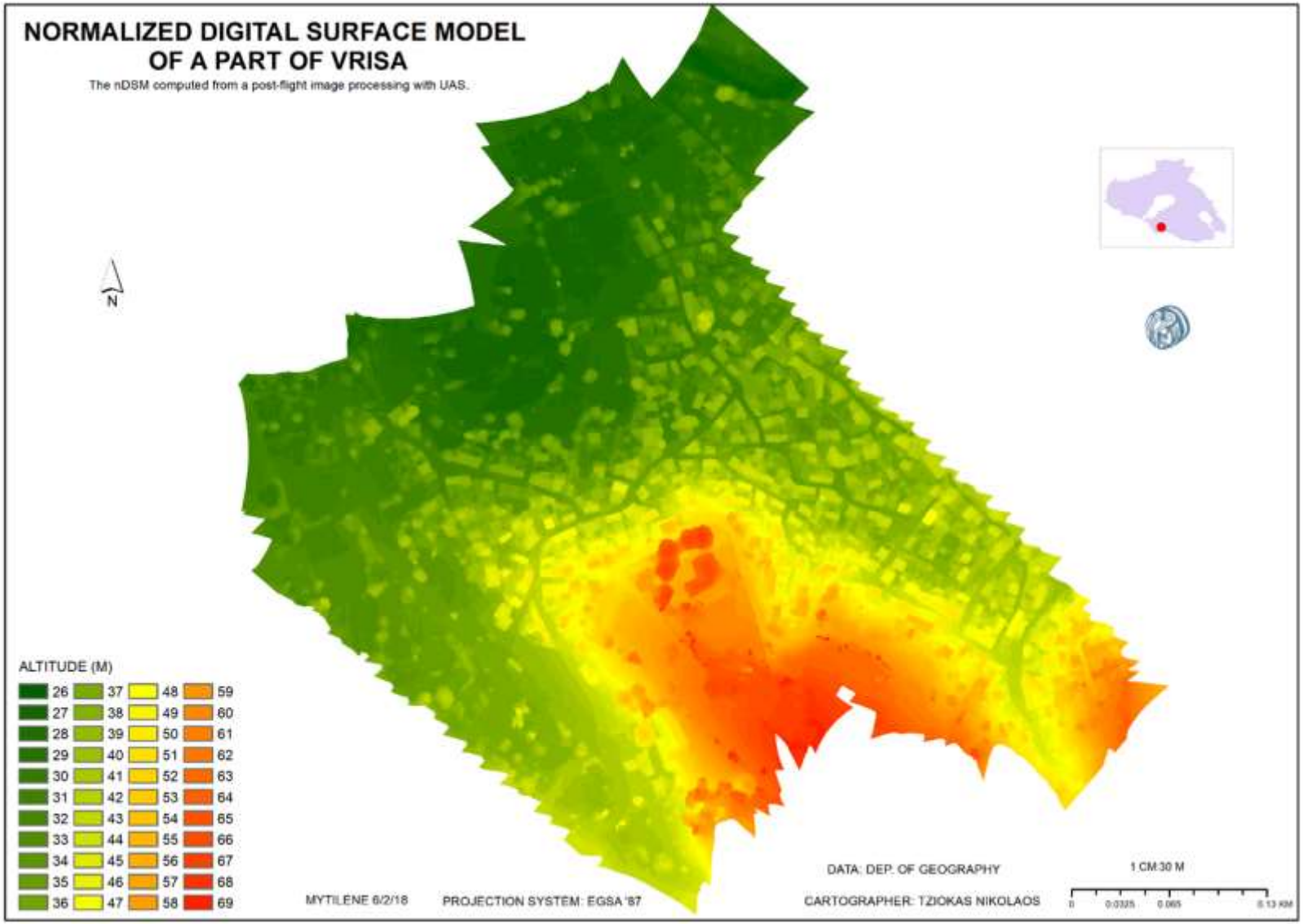

Map 1: nDSM of Vrysa with grid size is 5cm

Map 2: Multispectral orthophotomap of Vrysa. The spatial resolution is 5cm.

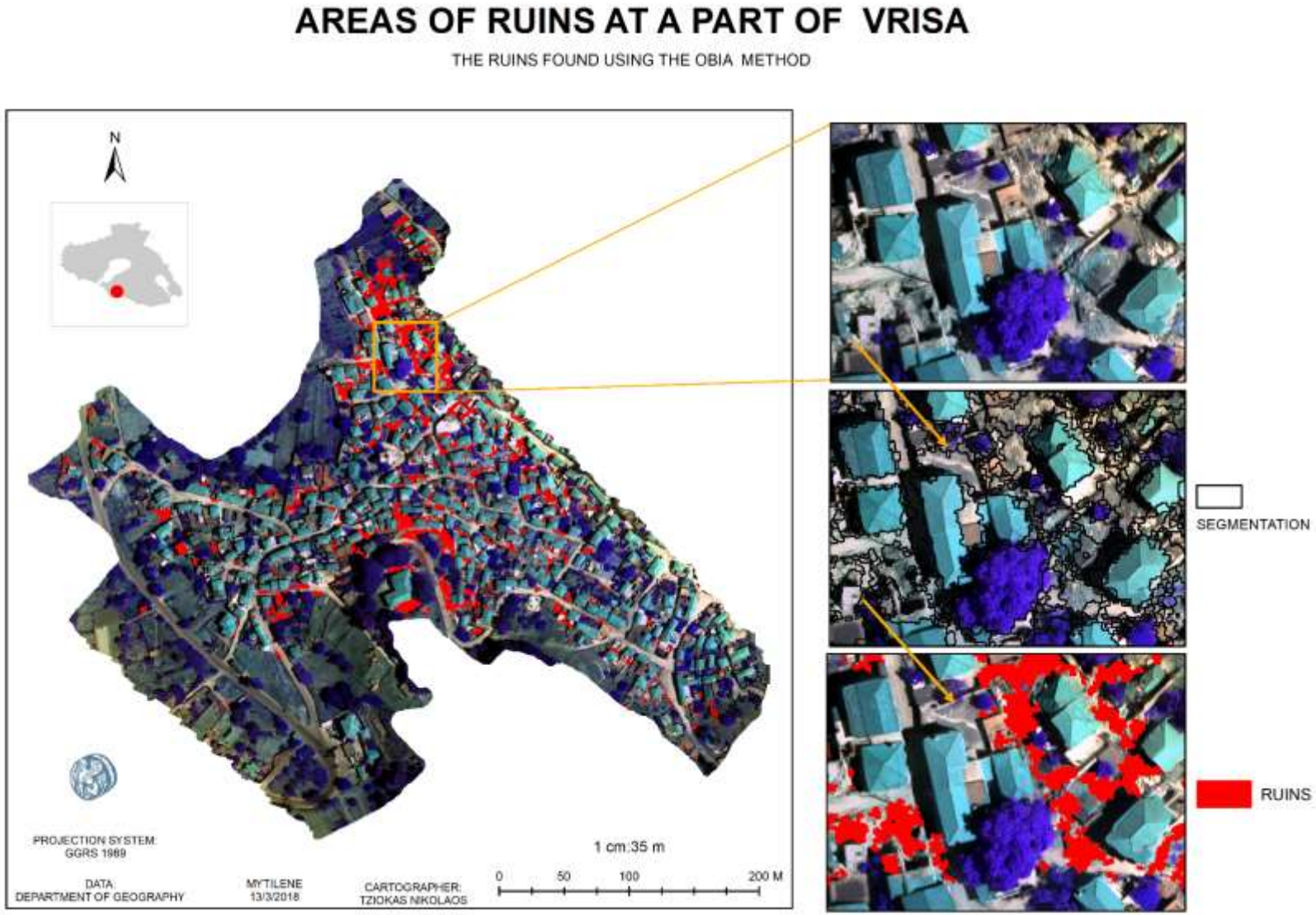

Map 3: Areas where the Ruins are